Journal of the Korean Physical Society, Vol. 71, No. 2, July 2017, pp. 111∼115

Growth of Epitaxial TiN (111) Thin Films with Low Resistivity on Si (111) by Crossed-Beam Pulsed Laser Deposition

Sukill Kang*
Institute of Photonics, Electronics, and Information, Department of Physics, Chonbuk National University, Jeonju 54896, Korea

C. M. Rouleau
Center for Nanophase Materials Sciences, Oak Ridge National Laboratory, Oak Ridge, Tennessee 37831, USA

(Received 25 May 2017, in final form 31 May 2017)

Titanium nitride (TiN) thin films were grown epitaxially on Si (111) substrates by reactive pulsed laser deposition. Substrate temperatures ranged from 550 to 950 °C while plume kinetic energies ranged from 46 to 154 eV. Quality of the grown films depended strongly on kinetic energy of the films than the growth temperatures. High quality film was grown at 750 °C with a laser plume kinetic energy of $\sim$ 92 eV. Full width at half maximum for a ω-scan around the TiN (111) peak and a φ-scan through the TiN (002) peak were 0.3° and 0.43°, respectively. The resistivity of the films was increased with increased temperatures and a room temperature resistivity of 3.8 $\mu\Omega$-cm was obtained.

PACS numbers: 81.15.Fg, 73.61.-r, 68.55.-a
Keywords: PLD, Resistivity, TiN
DOI: 10.3938/jkps.71.111

I. INTRODUCTION

TiN is an attractive material for semiconductor thin-film devices since its excellent properties include high electrical conductivity, high surface hardness, high melting point, and good wear resistance. TiN thin films have various applications such as diffusion barriers, contact metallizations in semiconductor devices and, when grown very thin, transparent conducting electrodes for flat panel displays. TiN may even serve as a buffer layer for GaN/Si (111) heterostructures because TiN is chemically similar to GaN. Such a buffer layer is technologically important since it would provide a means of integrating Si-based electronics with GaN-based optoelectronic devices [1].

TiN films have been grown by various techniques including chemical vapor deposition (CVD) [2], magnetron sputtering [3], atomic layer deposition (ALD) [4,5], and pulsed laser deposition (PLD) [6]. Commonly available target materials for PLD are usually hot-pressed sintered compound targets which sometimes deteriorate the quality of grown films because of low purity and density. For binary compounds, these problems can be overcome completely by ablating a melt-cast high purity elemental metal target through a high purity reactive gas. Willmott *et al.* have refined the approach and have introduced reactive crossed-beam PLD method, a nonequilibrium energetic-beam-assisted growth, to grow TiN (100) on Si (100) [7]. Not only does the method promote a region of highly dense mixing where the plume and the molecular beam cross, followed by a nearly collisionless expansion of the activated species toward the substrate, but because of the low time-averaged background pressure in the chamber, the substrate is not exposed to high impurity partial pressures as would be the case in the static pressure technique.

In this work, we report the growth of high quality TiN (111) thin films on Si (111) by reactive crossed-beam pulsed laser deposition using a conventional PLD chamber adapted for the reactive crossed-beam technique. It should be noticed that, in contrast to Willmott *et al.*, the ablation plume and pulsed jet crossed orthogonally in this work and the target was a standard metallic disk. To our knowledge, these TiN/Si (111) heterostructures are the best grown to date, as describe below.

II. EXPERIMENT

Thin films of TiN were grown on n-type Si (111) substrates (Resistivity 0.3 Ω-cm, 0.38 mm thick) by pulsed KrF laser ablation of a high purity Ti metallic target

*E-mail: skang@jbnu.ac.kr; Fax: +82-63-270-3320

 ©2017 The Korean Physical Society

through a supersonic N2 jet formed by a pulsed solenoid valve. The distance between the laser spot on the Ti target and pulsed valve nozzle was 1.3 cm and the Ti plume and pulsed N2 jet crossed orthogonally. The target-substrate separation, D_{ts}, was 5 cm. The chamber was equipped with an ion probe for measuring the time-of-flight (TOF) of the ablated species. The ion probe consisted of Kapton insulated coaxial cable (50 Ω impedance) placed in the path of the plume and biased negatively through an electrical feedthrough by an external bias supply. It was placed into the laser plume before growth to make TOF measurements. The voltage drop across an external resistor was captured as a function of time in synchronization with the laser flash. The trigger signal for synchronization was supplied by a fast photodiode placed behind a mirror in the beamline. To maximize the overlap between the Ti plume and the N_2 gas pulse, the delay between the laser trigger and pulsed valve driver trigger was adjusted until a maximum TOF was observed during ion probing (see Fig. 2 inset). For our apparatus, the optimum delay was found to be 315 μs for a corresponding pulsed valve driver gate width of 140 μs. As shown in the figure, the optimum delay was also independent of the initial mean kinetic energy imparted to the plume (*i.e.* vacuum TOF).

Vacuum TOFs for Ti ranging from 2.0 - 3.7 μs (corresponding to kinetic energies of 154 to 46 eV) were used for the depositions. Before deposition, the Si substrates were thermally cleaned in-situ at 900 °C. The oxide desorption process was monitored using in-situ reflection high energy electron diffraction (RHEED), which was also used to inspect the quality of the subsequent TiN layers. The chamber was pumped to 1×10^{-7} torr prior to deposition and the time averaged N_2 background pressure during deposition was 2×10^{-4} torr for all of the film-growth run. Depositions were carried out at substrate temperatures ranging from 550 to 950 °C as determined by infrared pyrometry and a total of 20,000 laser shots ($\sim$ 300 Å thick film) at 5 Hz repetition rate were used for each film growth. The Ti target was positioned 5 cm from the substrate and ablated at energy densities ranging from 1.7 $\sim$ 4.1 J/cm^2. Electrical measurements were performed using the custom made Hall effect measurement system.

III. RESULTS AND DISCUSSION

A characteristic RHEED pattern of a Si (111) surface was routinely observed along the <110> azimuth of Si immediately after thermal cleaning at 900 °C. Specifically, a sharp streaky diffraction pattern with Kikuchi lines developed and indicated oxide desorption and a well ordered (11) reconstructed Si (111) surface. Subsequent RHEED patterns of the TiN films were all sharp and streaky but diffraction spots were also present. For example, after 500 shots ($\sim$ 1.8 monolayers) for the TiN film grown at 750 °C with a 2.6 μs TOF (E_k = 91.7 eV), the RHEED pattern showed a two-dimensional growth mode. However, diffraction spots began to appear after 1,000 shots, indicating TiN film growth was more three dimensional. A reconstructed (22) surface structure was observed after 20,000 shots. This structure during the film growth was generally believed to arise from the unintentional presence of foreign atom species on the surface. There was a report that a (22) reconstructed TiN surface was due to O_2 contamination [8].

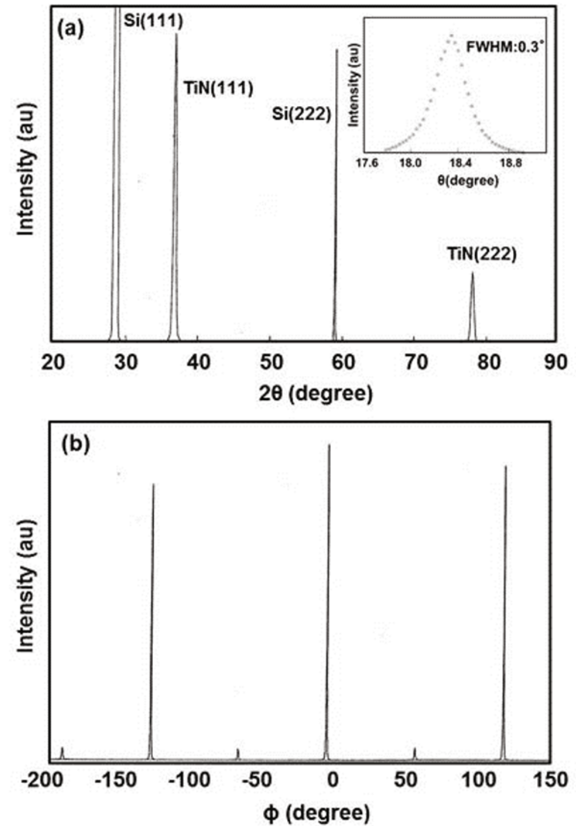

Fig. 1. (a) X-ray diffraction -2 scan result of a 300 Å TiN film grown on Si (111). The inset shows the X-ray rocking curve around the TiN (111) pole. (b) X-ray diffraction through the TiN (200) pole showing strong 3-fold symmetry.

Figure 1(a) shows a θ-2θ x-ray diffraction pattern of TiN thin film deposited on Si (111) at 750 °C with a 2.6 μs TOF. The diffraction pattern contained only the Si (111) and TiN (111) families and indicated that the TiN film was highly oriented along the (111) direction and essentially phase-pure. The lattice constants were found to be $a_0(\perp)$ = 4.236 Å and $a_0(\|)$ = 4.241 Å (bulk TiN a_0 = 4.242 Å) and this result indicated that the film was under in-plane tension with a tetragonal distortion of 0.0012. This is in agreement with the effective lattice mismatch when coincidence epitaxy is considered (5 TiN units on 4 Si units = -2.51% mismatch). The inset shows an x-ray rocking curve of the TiN (111) reflection with a full width at half maximum (FWHM) of

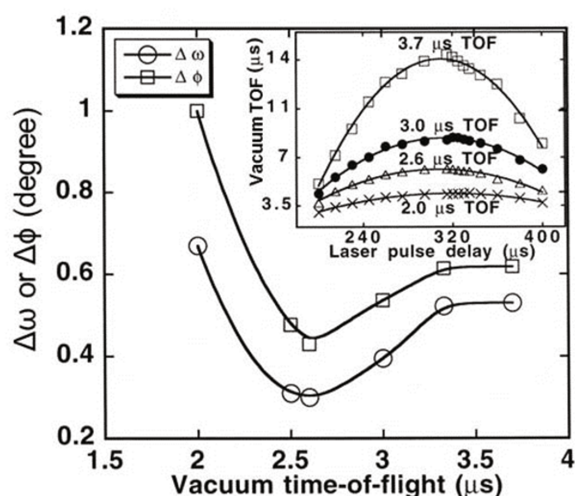

Fig. 2. Rocking curve width for the TiN (111) reflection and mosaic spread for the TiN (200) pole as a function of energy imparted to the plume. The inset shows that the maximum plume/gas pulse overlap occurs at $\sim$ 315 μs and is not a function of the energy imparted to the plume. Only the curvature changes with vacuum TOF.

0.3° which indicates excellent out-of-plane texture. This value is much lower than previously reported for TiN (111)/Si (111) [9], and is even better than the rocking curve width reported for TiN (111) grown on 6H-SiC (0001) [10]. Figure 1(b) shows a φ-scan result through the 200 reflection of the TiN film. Although peaks occur every 60°, the film can be considered to be essentially a single crystallographic domain since there is such a large difference (more than 1,000 $\times$) between peak intensities. The largest peaks occur every 120° and overlap those of the Si substrate which indicates excellent in-plane registry. The mosaic spread in the φ-scan for this film was 0.43° and the in-plane orientation relationships between all the TiN films and the underlying Si substrates were TiN [200] || Si [200] and TiN [111] || Si [111].

The dependence of the FWHM of the x-ray rocking curve on ablation plume kinetic energy (*i.e.* the Ti vacuum TOF) was investigated and is shown in Fig. 2. It was found that the FWHM of the rocking curve and of the φ-scan decreased as the TOF increased from 2.0 μs to 2.6 μs, and then both increased again as the TOF increased from 2.6 μs to 3.7 μs. However this trend did not result from the plume “missing” the gas pulse as the vacuum TOF was varied. As shown in the inset of Fig. 2, maximum overlap conditions were largely independent of the energy imparted to the plume (*i.e.* vacuum TOF), mainly because the TOF is so much shorter than the laser pulse delay. However, the effect of the gas pulse on the plume varied strongly with vacuum TOF as shown by the increasing curvature as vacuum TOF increases.

The TiN thin films grown on Si (111) with shorter TOFs ranging from 2.0 to 2.5 μs exhibit smooth surfaces except for the presence of some cracks and small round particles. Figure 3(a) is a SEM micrograph of a TiN film grown at 750 °C with a 2.0 μs TOF showing the cracks and small particles. The cracks and particulates most likely resulted from the high energy density (short TOF) employed for this film - cracks resulting from the high residual strains caused by the very energetic species impinging on the growing film and particulates possibly resulting from hot molten droplets ejected from the target. Cracks also are favored due to the difference in thermal expansion coefficients between TiN and Si (TiN = 4.7 $\times$ 10^{-6} K^{-1}, Si = 3.6 $\times$ 10^{-6} K^{-1}). Ex situ examination of the Ti target surface showed deep cone-shaped craters after 5,000 laser shots which supports the idea that massive amounts of material are ejected for this TOF. Even with target rotation, target surface roughening was accelerated by long-term exposure to laser irradiation. Films grown in this regime exhibited a 38 - 50 Å RMS surface roughness over a 10 μm $\times$ 10 μm scan

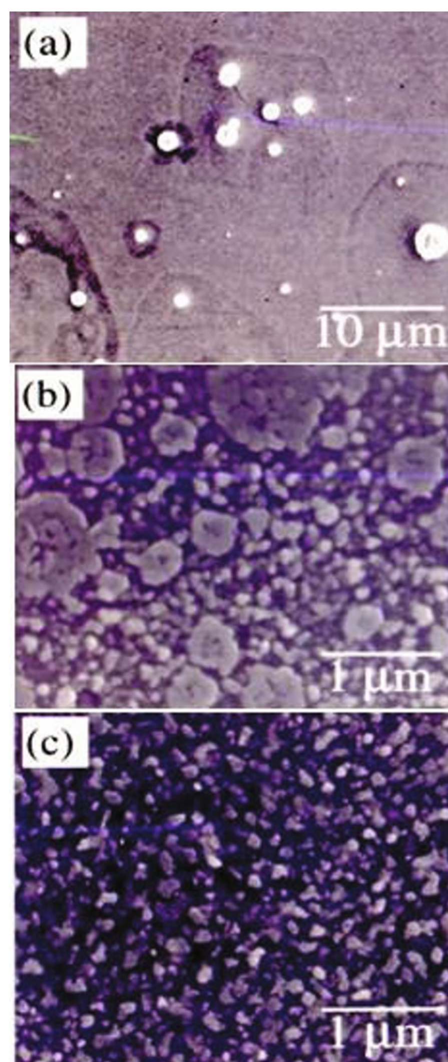

Fig. 3. (Color online) SEM images of 300 Å TiN films grown on Si (111) at vacuum TOF (a) 2.0 μs (b) 2.6 μs, and (c) 3.7 μs.

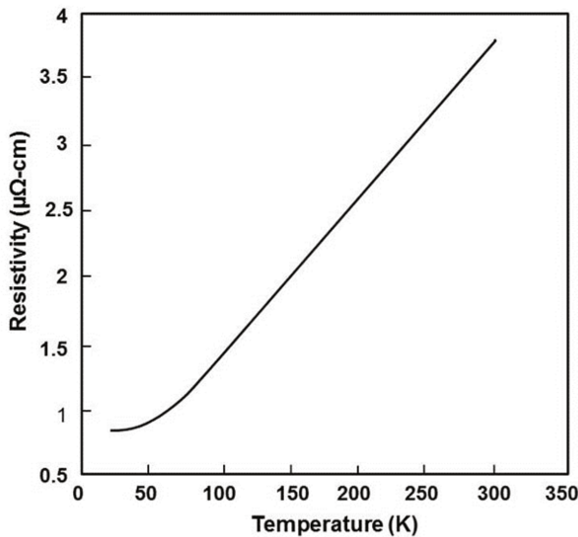

Fig. 4. Temperature dependent resistivity of a TiN film grown at 750 °C with 2.6 μs TOF.

(measured by AFM).

In contrast to the smooth, cracked and decorated surfaces obtained at short TOFs, Fig. 3(b) shows a SEM micrograph of a TiN film grown with a 2.6 μs vacuum TOF (E_k = 91.7 eV), the value considered to be optimal. When also contrasted with a film grown at higher vacuum TOF, Fig. 3(c), the optimal film's morphology clearly shows a mixed nature that might result as follows. For some fixed temperature and at short vacuum TOFs, the energy-dependent gas pulse collision cross-section is too small and the impinging growth-species are left too energetic to allow complete long-range order to develop and consequently, highly stressed and somewhat disordered films result. Conversely, at sufficiently long vacuum TOFs the energy-dependent gas pulse collision cross-section is much larger and extreme collisional-slowing and/or condensation of the plume might occur leading to a columnar grain microstructure that is essentially homogeneous, as shown in Fig. 3(c), because too few energetic species are present to erode unfavorable grains or provide sufficient mobility to planerize the surface. Thus, at some intermediate TOF the energetics are favorable to balance the forces favoring film damage and erosion against those favoring highly three-dimensional growth. However, we note that the ablation plume's kinetic energy distribution is broad and even when the most probable kinetic energy is tuned to the optimal value ($\sim$ 92 eV), the incident flux contains Ti atoms/ions with both higher and lower kinetic energies, rendering the optimal films still imperfect. If this is correct, then growth using more nearly mono energetic Ti source, such would be expected to produce high quality TiN.

Electrical resistivity measurements were performed using the Van der Pauw method with indium contacts. The temperature-dependent resistivity of a film grown at 750 °C with a 2.6 μs TOF was measured from 10 K to 300 K and is shown in Fig. 4. The higher temperature portion of the curve (T $\geq$ 75K) varied as T with a slope equal to 0.01195 $\mu\Omega$-cm/K and indicated metallic behavior. The lowest room-temperature resistivity was found to be 3.8 $\mu\Omega$-cm, which is very promising for contact metallization in advanced microelectronic devices, since this value is lower than any previously reported [9, 11, 12]. The resistivity was observed to decrease as growth temperatures increased, while increasing resistivity was observed for increasing TOFs. Generally, the resistivity was affected by preferred orientation, impurity content, microstructure of the film. Since impurities were not detected from EDX analysis, the changes in resistivity are considered to be due to diffuse scattering of electrons from the film surface and grain boundary scattering [9]. This conclusion is not unreasonable given the microstructures present in Fig. 3.

IV. CONCLUSION

In conclusion, we have grown high quality 300 Å thick epitaxial TiN thin films on Si (111) by reactive crossed-beam pulsed laser deposition. The crystallinity and surface morphology of the films were dependent strongly on the kinetic energy of the ablated Ti plume (as measured by vacuum TOF) and weakly dependent on the growth temperature. With optimal TOF (2.6 μs) and temperature (750 °C), high quality in-plane-aligned TiN thin films were obtained with x-ray rocking curve and φ-scan mosaic spreads equal to $\Delta\omega_{111} = 0.3°$ and $\Delta\varphi_{200} = 0.43°$, respectively. Under optimum conditions, films with room temperature resistivities as low as 3.8 $\mu\Omega$-cm were obtained. These are the lowest values reported to date for growth of TiN on Si (111).

ACKNOWLEDGMENTS

This paper was supported by research funds of Chonbuk National University in 2014.

REFERENCES

[1] L. Li, R. Nakamura, Q. Wang, Y. Jiang and J. Ao, Nanoscale Res. Lett. **9**, 590 (2014).

[2] G. Zhao, T. Zhang, T. Zhang, J. Wang and G. Han, J. Non-cryst. Sol. **354**, 1272 (2008).

[3] Y. L. Jeyachandran, S. K. Narayandass, D. Mangalaraj, S. Areva and J. A. Mielczarski, Mater. Sci. & Eng. A **445**, 223 (2007).

[4] M. Burke, A. Blake, I. M. Povey, M. Schmidt, N. Petkov, P. Carolan and A. J. Quinn, J. Vac. Sci. Technol. A **32**, 031506 (2014).

[5] H. Van Bui, A. Y. Kovalgin and R. A. M. Wolters, ECS J. Solid State Sci. Technol. **1**, 285 (2012).
[6] M. Bonholzer, M. Lorenz and M. Grundmann, Phys. Status Solidi A **211**, 2621 (2014).
[7] P. R. Willmott, R. Timm and J. R. Huber, J. Appl. Phys. **82**, 2082 (1997).
[8] L. Hultman, H. Ljungcrantz, C. Hallin, E. Janzen, J-E. Sundgren, B. Pecz and L. R. Wallenberg, J. Mat. Res. **11**, 2458 (1996).
[9] K. Sano, M. Oose and T. Kawakubo, Jpn. J. Appl. Phys. **34**, 3266 (1995).
[10] A. A. Iliadis, S. N. Andronescu, K. Edinger, J. H. Orloff, R. D. Vispute, V. Talyanky, R. P. Sharma, T. Venkatesan, M. C. Wood and K. A. Jones, Appl. Phys. Lett. **73**, 3545 (1998).
[11] W. Uen, Z. Li, S. Lan, T. Yang and S. Liao, Thin Solid Films **516**, 99 (2007).
[12] W. Chen, C. Peng and L. Chang, Nanoscale Res. Lett. **9**, 551 (2014).